Open-charm axial-vector and tensor meson resonances from Lattice QCD

LATTICE 2024, Liverpool

Nicolas Lang[a], David Wilson[b]

1st of August 2024

[a]Universitat de Valencia, IFIC
[b]University of Cambridge

The D-meson spectrum

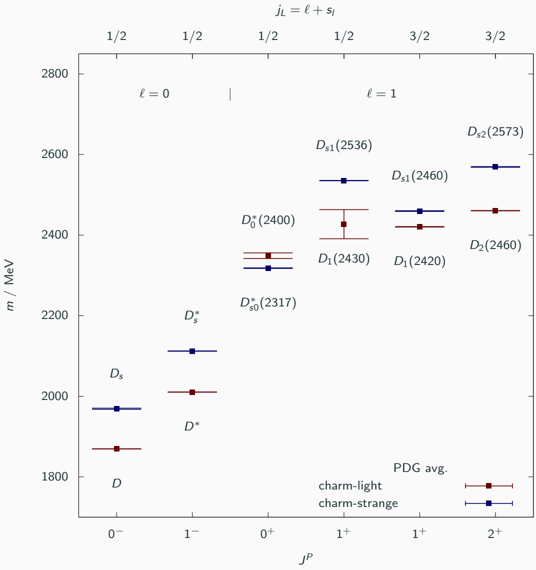

[Particle masses from PDG]

Outline and ensemble details

In this talk I...

- review previous analyses of the scalar resonances in $D\pi$ and DK amplitudes
- present our work on axial-vector and tensor D-meson states in $I = \frac{1}{2}$ $D^*\pi$ amplitudes

Ensemble details

a_s:	0.12 fm
a_t^{-1}:	5.667 GeV
$(L/a_s)^3 \times (T/a_t) \in$	$\{16^3, 20^3, 24^3\} \times 128$
m_π:	391 MeV
N_f:	$2+1$
N_{cfg}:	$\{479, 603, 552\}$
$N_{\text{t-srcs}}$:	$\{4, 1-4, 1-4\}$

Spectrum computation

Distillation [Peardon et al., 2009]:

- Distillation operator:

$$\left[\Box(t)\right]_{xy} = \left[V(t)V^{\dagger}(t)\right]_{xy} = \sum_{k=1}^{N} v_x^{(k)}(t) v_y^{(k)\dagger}(t)$$

- Distillation space objects:

$$\phi^X_{\alpha\beta}(t) = V^{\dagger}(t)\Gamma^X_{\alpha\beta}(t)V(t)$$

$$\tau_{\alpha\beta}(t', t) = V^{\dagger}(t')M^{-1}_{\alpha\beta}(t', t)V(t)$$

Variational method:

- Correlator matrix (large basis of operators!):

$$C_{ij}(t) = \langle 0|\mathcal{O}_i(t)\mathcal{O}_j^{\dagger}(0)|0\rangle \,,$$

- Find "optimal" interpolators by solving Generalised Eigenvalue (GEV) problem

$$C_{ij}(t)v_j^{(\mathfrak{n})} = \lambda_{\mathfrak{n}}(t, t_0)C_{ij}(t_0)v_j^{(\mathfrak{n})},$$

$$\Omega_n^{\dagger} \equiv \sum_{i=1}^{N} v_i^n \mathcal{O}_i^{\dagger}$$

- Fit Principal correlators (eigenvalues):

$$\lambda_{\mathfrak{n}}(t, t_0) = (1 - A_{\mathfrak{n}})e^{-E_{\mathfrak{n}}(t-t_0)} + A_{\mathfrak{n}}e^{-E'_{\mathfrak{n}}(t-t_0)}$$

Meson operator bases

- Quark bilinears:

$$\bar{q}(\vec{x},t)\boldsymbol{\Gamma}_t^{Jm} q(\vec{x},t)$$

- Single mesons with definite flavour and momentum:

$$\mathcal{O}^{\dagger\,Jm}_{\boldsymbol{F}\nu}(\vec{p},t) = \sum_{\vec{x}} e^{i\vec{p}\cdot\vec{x}} \sum_{\nu_1,\nu_2} \mathcal{C}_{\mathrm{SU(3)}} \begin{pmatrix} \bar{\mathbf{3}} & \mathbf{3} \text{ or } \mathbf{1} & \boldsymbol{F} \\ \nu_1 & \nu_2 & \nu \end{pmatrix} \bar{q}_{\nu_1}(\vec{x},t)\boldsymbol{\Gamma}_t^{Jm} q_{\nu_2}(\vec{x},t)$$

- Meson-meson:

$$\begin{aligned} &\Omega^{\dagger\,Jm}_{\boldsymbol{F}\nu}(\vec{P},t;[p_1,p_2]) = \\ &\quad \sum_{\substack{\nu_1,\nu_2\\ m_1,m_2}} \mathcal{C}_{\mathrm{SU(3)}} \begin{pmatrix} \boldsymbol{F}_1 & \boldsymbol{F}_2 & \boldsymbol{F} \\ \nu_1 & \nu_2 & \nu \end{pmatrix} \mathcal{C} \begin{pmatrix} J_1 & J_2 & J \\ m_1 & m_2 & m \end{pmatrix} \\ &\quad \times \sum_{\substack{\vec{p}_i \in \{\, \vec{p}_i \,\}^* \\ \vec{p}_1 + \vec{p}_2 = \vec{P}}} \Omega^{\dagger\,J_1 m_1;}_{1\,\boldsymbol{F}_1\nu_1}(\vec{p}_1,t)\,\Omega^{\dagger\,J_2 m_2;}_{2\,\boldsymbol{F}_2\nu_2}(\vec{p}_2,t) \end{aligned}$$

Ω_i are variationally optimal operators

Lattice symmetries

Continuum: Poincaré symmetry
Lattice: lattice translations and (subgroups of) cubic group

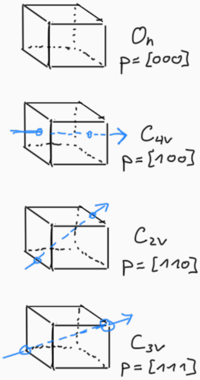

- Irrep of continuum rotation group is reducible representation of O_h (and subgroups)
- Can expand $\mathcal{O}^{Jm}$ in irreps of O_h (or subgroups)
- Inverting this expansion defines subduction to lattice irreps:

$$\mathcal{O}^{\dagger\,\Lambda\mu;[J]}_{\boldsymbol{F}\nu}(\vec{p},t) = \sum_m \mathcal{S}^{J,m}_{\Lambda,\mu}\mathcal{O}^{\dagger\,Jm}_{\boldsymbol{F}\nu}(\vec{p},t)$$

Subduced meson-meson operator:

$$\mathcal{O}^{\dagger\,\Lambda\mu}_{\boldsymbol{F}\nu}(\vec{P},t;[p_1,p_2]) = \sum_{\substack{\nu_1,\nu_2\\ \mu_1,\mu_2}} \mathcal{C}_{\mathrm{SU(3)}}\begin{pmatrix} \boldsymbol{F}_1 & \boldsymbol{F}_2 & \boldsymbol{F} \\ \nu_1 & \nu_2 & \nu \end{pmatrix} \mathbb{C}\begin{pmatrix} \Lambda_1^{\vec{p}_1} & \Lambda_2^{\vec{p}_2} & \Lambda^{\vec{P}} \\ \mu_1 & \mu_2 & \mu \end{pmatrix}$$

$$\times \sum_{\substack{\vec{p}_i \in \{\,\vec{p}_i\,\}^* \\ \vec{p}_1+\vec{p}_2=\vec{P}}} \mathcal{O}^{\dagger\,\Lambda_1\mu_1;}_{1\,\boldsymbol{F}_1\nu_1}(\vec{p}_1,t)\,\mathcal{O}^{\dagger\,\Lambda_2\mu_2;}_{2\,\boldsymbol{F}_2\nu_2}(\vec{p}_2,t)$$

Zero-momentum subductions

$\vec{d}$	G	Λ	J^P $(\vec{P}=\vec{0})$ $\lvert\lambda\rvert^{(\tilde{\eta})}$ $(\vec{P}\neq\vec{0})$	${}^1\ell_J$	${}^3\ell_J$
[000]	O_h	A_1^+	0^+, ...	${}^1S_0$	
		A_2^+	3^+, ...		${}^3D_3$
		E^+	2^+, ...	${}^1D_2$	${}^3D_2$
		T_1^+	1^+, 3^+, ...		$({}^3S_1, {}^3D_1)$, ${}^3D_3$
		T_2^+	2^+, 3^+, ...	${}^1D_2$	${}^3D_2$, ${}^3D_3$
		A_1^-	0^-, ...		${}^3P_0$
		A_2^-	3^-, ...	...	...
		E^-	2^-, ...		${}^3P_2$
		T_1^-	1^-, 3^-, ...	${}^1P_1$	${}^3P_1$
		T_2^-	2^-, 3^- ...		${}^3P_2$

O_h: Lattice symmetry group at rest

From FV spectrum to scattering amplitudes

Quantisation condition

$$\det\left[\mathbf{1} + i\boldsymbol{\rho}(s)\cdot\boldsymbol{t}(s)\cdot\left(\mathbf{1} + i\boldsymbol{\mathcal{M}}(s,L)\right)\right] = 0$$

[Original derivation: M. Lüscher; many extensions e.g. Sharpe, Briceño...]

- Holds for arbitrary $2 \to 2$ scattering
- $\rho(s) = 2k(s)/\sqrt{s}$ with $k(s)$ the COM-momentum function and $s = E_{\mathrm{CM}}^2$
- $\boldsymbol{t}(s)$ = infinite volume t-matrix
- $\boldsymbol{\mathcal{M}}(s,L))$ encodes finite-volume effects
- $\boldsymbol{t}(s)$ is diagonal in total angular momentum J
- $\boldsymbol{\mathcal{M}}(s,L))$ is dense in J

Fitting and pole-finding

Procedure:

- Parameterise the amplitude
- Determine the finite-volume spectrum from the determinant condition
- Compare the spectrum to the lattice result
- Change parameters and iterate to minimize the χ^2
  (using favourite numerical minimisation procedure)

The finite-volume formalism does not give us a functional form for the amplitude. We need a parametrisation and want to put as much prior knowledge into it without making assumptions about the dynamics.

Dynamics-independent amplitude constraints

- Unitarity: K matrix

$$\boldsymbol{t} = \boldsymbol{K}(1 - i\boldsymbol{\rho}\boldsymbol{K})^{-1}$$

- Rotational symmetry: The partial-wave projection

$$(\boldsymbol{t}^{-1})_{alS,bl'S'}(s) = (\boldsymbol{K}^{-1})_{alS,bl'S'} - i\rho_a \delta_{ll'}\delta_{SS'}$$

- Angular-momentum barrier: threshold factors

$$(\boldsymbol{t}^{-1})_{alS,bl'S'}(s) = (2k_{\text{cm}}^{(a)})^{-l}(\boldsymbol{K}^{-1})_{alS,bl'S'}(2k_{\text{cm}}^{(b)})^{-l'} - i\rho_a \delta_{ll'}\delta_{SS'}$$

- Analyticity: Chew-Mandelstam phase space

$$I(s) = I(s_{\mathrm{thr}}) + \frac{\rho}{\pi}\log\left[\frac{\xi + \rho(s)}{\xi(s) - \rho(s)}\right] - \frac{\xi(s)}{\pi}\frac{m_1 - m_2}{m_1 + m_2}\log\frac{m_2}{m_1}$$

with $\xi(s) = 1 - \frac{(m_1+m_2)^2}{s}$; subtracted at threshold

Review: $D\pi$ at $m_\pi = 239$ MeV and $m_\pi = 391$ MeV

Single pole at both masses:

- $t \sim \frac{c^2}{s_{\text{pole}} - s}$
  $\sqrt{s} = m \pm \frac{i}{2}\Gamma$
- @$m_\pi = 391$ MeV:
  shallow bound-state
  $\approx 2 \pm 1$ MeV below threshold
- @$m_\pi = 239$ MeV: resonance
  $\approx 77 \pm 64$ MeV above threshold;
  below PDG value
  $\Gamma = 425 \pm 224$ MeV
- Strong coupling to $D\pi$ channel in both studies

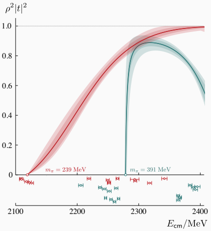

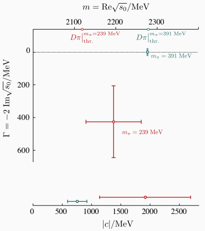

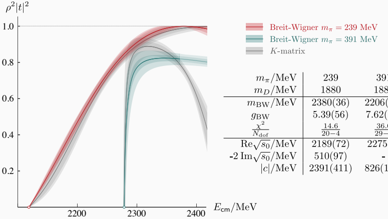

m_π/MeV	239	391
m_D/MeV	1880	1887
m_{BW}/MeV	2380(36)	2206(32)
g_{BW}	5.39(56)	7.62(75)
$\frac{\chi^2}{N_{\text{dof}}}$	$\frac{14.6}{20-4}$	$\frac{36.0}{29-5}$
$\text{Re}\sqrt{s_0}$/MeV	2189(72)	2275(1)
-2 $\text{Im}\sqrt{s_0}$/MeV	510(97)	-
$\|c\|$/MeV	2391(411)	826(133)

$$m_\pi = 239\ \text{MeV}: \sqrt{s_0}/\text{MeV} = (2196 \pm 64) - \frac{i}{2}(425 \pm 224); \quad |c_{D\pi}|/\text{MeV} = 1916 \pm 776$$

$$m_\pi = 391\ \text{MeV}: \sqrt{s_0}/\text{MeV} = 2275.9 \pm 0.9; \quad |c_{D\pi}|/\text{MeV} = 550 \pm 160$$

[L. Gayer, N. Lang et al (HadSpec), arXiv:2102.04973]
[G. Moir et al (HadSpec), JHEP 10 (2016) 011]

Review: $I = 0$ DK at $m_\pi = 239$ MeV and $m_\pi = 391$ MeV

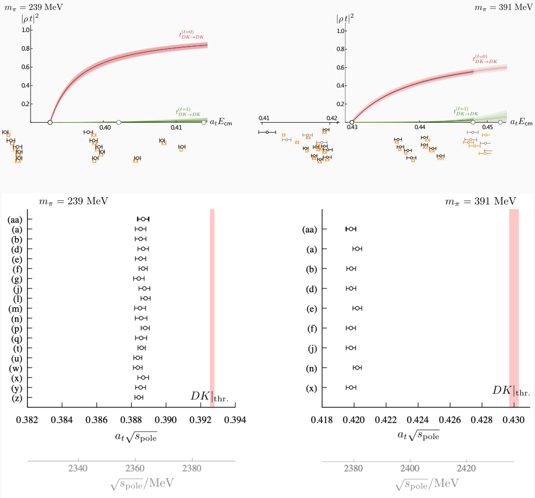

Bound states at both masses

$m_\pi = 239$ MeV: $\sqrt{s} = 2362(3)$ MeV; $|c| = 1420(50)$ MeV
$m_\pi = 391$ MeV: $\sqrt{s} = 2380(3)$ MeV; $|c| = 1730(110)$ MeV

[G. Cheung et al (HadSpec), JHEP 02 (2021) 100 arXiv: 2008.06432]

Review: $D\pi$ and DK

Conclusions from $D\pi$ and DK:

- *Expected* order of states: D_0^* lighter than D_{s0}^*
- Weak dependence on light-quark mass of charm-strange states
- some light-quark mass dependence in the charm-light states
- $u\chi_{PT}$: many predictions of two-pole structure in S-wave amplitudes. Higher sextet pole? Insufficient data here for a reliable extraction.

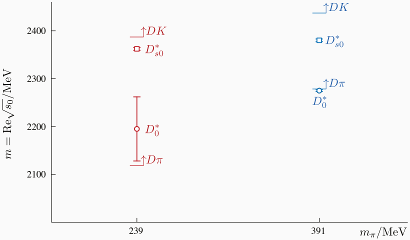

Heavy-light mesons with spin: $D^*\pi \to D^*\pi$ Spectra

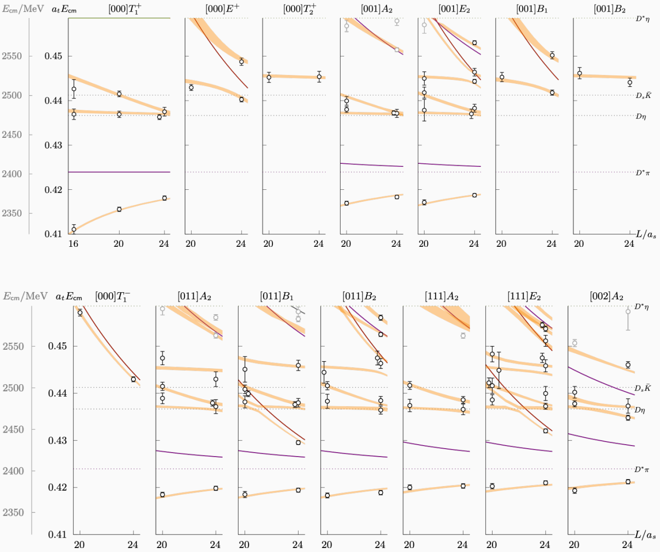

[N. Lang and D. Wilson (HadSpec) arXiv: 2205.05026]

$D^*\pi \to D^*\pi$ amplitude parametrisations

Slightly more complicated:

- Several resonances in $J^P = 1^+$

$$K_{ij} = \frac{g_{0,i}g_{0,j}}{m_0^2 - s} + \frac{g_{1,i}g_{1,j}}{m_1^2 - s} + \gamma_{ij}$$

- Partial-wave mixing between $^3S_1$ and $^3D_1$

$$K_{J^P=1^+} = \begin{bmatrix} K_{D^*\pi\{^3S_1\}} & K_{D^*\pi\{^3S_1 \leftrightarrow {}^3D_1\}} \\ & K_{D^*\pi\{^3D_1\}} \end{bmatrix} .$$

- Mixing between $D\pi\{^1D_2\}$ and $D^*\pi\{^3D_2\}$ amplitudes of $J^P = 2^+$

$$K_{J^P=2^+} = \begin{bmatrix} K_{D\pi\{^1D_2\}} & K_{D\pi\{^1D_2\} \leftrightarrow D^*\pi\{^3D_2\}} \\ & K_{D^*\pi\{^3D_2\}} \end{bmatrix} .$$

- Various negative-parity background processes in non-zero momentum irreps which are considered in the K matrix with terms constant in s

$D^*\pi \to D^*\pi$ (Amplitudes)

$m_\pi = 391$ MeV

$$\begin{aligned}
m_0 &= (0.42294 \pm 0.00017 \pm 0.00011) \cdot a_t^{-1} \\
m_1 &= (0.43691 \pm 0.00028 \pm 0.00006) \cdot a_t^{-1} \\
g_0(^3S_1) &= (0.528 \pm 0.022 \pm 0.022) \cdot a_t^{-1} \\
g_0(^3D_1) &= (0.390 \pm 0.850 \pm 0.089) \cdot a_t \\
g_1(^3S_1) &= (0.014 \pm 0.012 \pm 0.002) \cdot a_t^{-1} \\
g_1(^3D_1) &= (-6.40 \pm 1.36 \pm 0.21) \cdot a_t \\
\gamma(^3S_1 \to {}^3S_1) &= (10.3 \pm 1.2 \pm 0.6)
\end{aligned}$$

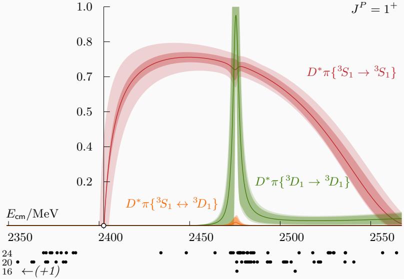

$$\begin{aligned}
m_2 &= (0.44546 \pm 0.00029 \pm 0.00006) \cdot a_t^{-1} \\
g_2(^1D_2) &= (1.730 \pm 0.065 \pm 0.013) \cdot a_t \\
g_2(^3D_2) &= (3.02 \pm 0.92 \pm 0.09) \cdot a_t \\
\gamma(^1D_2 \to {}^1D_2) &= (222 \pm 172 \pm 225) \cdot a_t^4
\end{aligned}$$

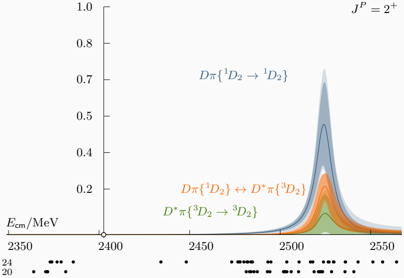

$$\chi^2/N_{\rm dof} = \frac{95.0}{94-15} = 1.20$$

[N. Lang and D. Wilson (HadSpec) arXiv: 2205.05026]

Poles and couplings (MeV)

D_1 $\quad \sqrt{s} = 2397(2)$ $\quad |c_{D^*\pi\{^3S_1\}}| = 1007(123)$ $\quad |c_{D^*\pi\{^3D_1\}}| = 2(3)$

D_1' $\quad \sqrt{s} = (2475(3) - \frac{i}{2}5(3))$ $\quad |c_{D^*\pi\{^3S_1\}}| = 32(33)$ $\quad |c_{D^*\pi\{^3D_1\}}| = 239(77)$

D_2^* $\quad \sqrt{s_{D_2}} = (2524(2) - \frac{i}{2}10(4))$ $\quad |c_{D\pi\{^1D_2\}}| = 234(11)$ $\quad |c_{D^*\pi\{^3D_2\}}| = 137(126)$

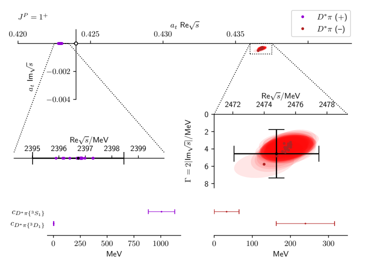

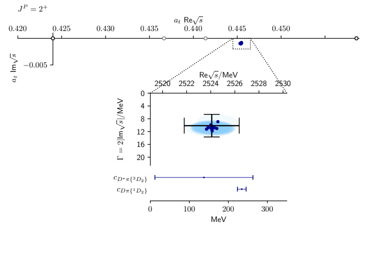

Heavy-quark spin symmetry (HQSS)

Heavy-quark (HQ) limit: $m_c \to \infty$

- HQ spin decouples from dynamics
- Heavy-light mesons form degenerate doublets

$$J = J_L + s_H$$

$$J_L = \ell + s_L$$

Lowest D-meson excitations
(P-wave states in "quark-model picture"):

- $J_L = \frac{1}{2} \Rightarrow J^P \in \{0^+, 1^+\}$
- $J_L = \frac{3}{2} \Rightarrow J^P \in \{1^+, 2^+\}$

Consequences:

- Broad $D_1(2430)$ decays exclusively to S-wave
- Narrow $D_1(2420)$ decays exclusively to D-wave

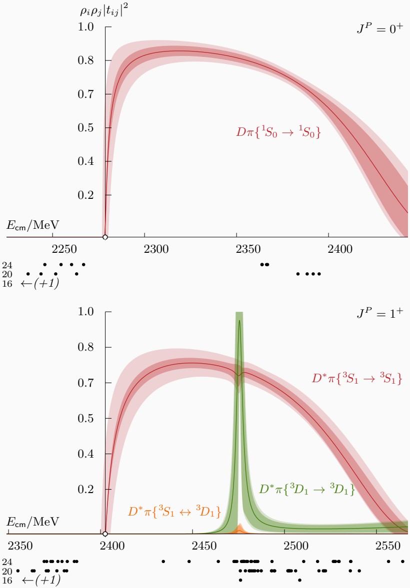

[N. Lang and D. Wilson (HadSpec) arXiv: 2205.05026]

Conclusions and Outlook

Conclusions from $D^*\pi \to D^*\pi$

- The mass of the bound D_1 is lower than the PDG value for the $D_1(2430)$ despite heavier-than-physical light quarks
- Strong coupling of the bound D_1 to $D^*\pi \to$ expect a broad resonance at physical point (as seen experimentally)
- Near-decoupling of the two D_1 states matches HQSS expectations

Outlook: coupled $D^*\pi$, $D^*\eta$ and $D_s^*\bar{K}$

- Analysis in final stages!
- Improved precision of 2^+ amplitudes
- Second pole in 1^+ amplitudes as conjectured by uχ_{PT}?
- Stay tuned!

Backup material

Lattice formulation of QCD

Start from QCD action:

$$S_{\text{QCD}} = \underbrace{\int d^4x \sum_{f=1}^{6} \sum_{a,b=1}^{3} \sum_{\alpha,\beta=0}^{3} \bar{q}^f_{\substack{a\\ \alpha}} (i \not{D}_{\substack{ab\\ \alpha\beta}} - m_f \delta_{ab} \delta_{\alpha\beta}) q^f_{\substack{b\\ \beta}}}_{S_F} - \underbrace{\int d^4x \sum_{i=1}^{8} \sum_{\mu,\nu=0}^{3} \frac{1}{4} G^i_{\mu\nu} G^{\mu\nu}_i}_{S_G}$$

Introduce set of lattice sites:

$$\Lambda = \{ x = an \mid n \in \{ 0, \dots L/a_s \}^3 \times \{ 0, \dots, T/a_t \} \}$$

Perform Wick rotation: $t \to -it$

a_t: temporal lattice spacing

a_s: spatial lattice spacing

T: time extent

L: spatial extent

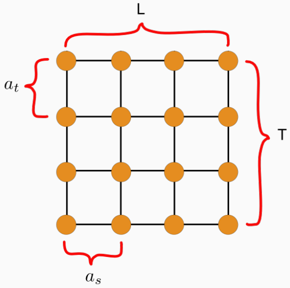

Discretization of gauge action

The Gluon part of the action is:

$$S_G = \int d^4x \sum_{i=1}^{8} \sum_{\mu,\nu=0}^{3} \frac{1}{4} G^i_{\mu\nu} G^{\mu\nu}_i$$

where

$$G^i_{\mu\nu} = \partial_\mu A^i_\nu - \partial_\nu A^i_\mu - f_{ijk} A^j_\mu A^k_\nu$$

Now replace:

$$A_\mu \to U_\mu(x) = \exp[iag_s A_\mu(x)]$$

Define Plaquette:

$$U_{\mu\nu}(x) = U_\mu(x) U_\nu(x + a\hat{\mu}) U^\dagger_\mu(x + a\hat{\nu}) U^\dagger_\nu(x)$$

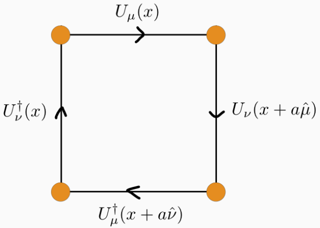

The discretized action can be written:

$$S_G[U] = \frac{2}{g^2} \sum_{x \in \Lambda} \sum_{\mu < \nu} \text{Re}\left\{\text{Tr}[\mathbf{1} - U_{\mu\nu}(x)]\right\}$$

For $a \to 0$ continuum expression is recovered

Discretization of fermion action

Fermion (Dirac) term is:

$$\int d^4x \sum_{f=1}^{6} \sum_{a,b=1}^{3} \sum_{\alpha,\beta=0}^{3} \bar{q}^f_{\substack{a \\ \alpha}} (i\not{D}_{\substack{ab \\ \alpha\beta}} - m_f \delta_{ab}\delta_{\alpha\beta}) q^f_{\substack{b \\ \beta}}$$

Naïve discretisation:

$$S_F \to a^4 \sum_f \sum_{x\in\Lambda} \bar{q}^f(x) \left(\sum_{\mu=1}^{4} \gamma_\mu \frac{U_\mu(x)\delta_{x+a\hat{\mu},y} - U^\dagger_\mu(x-a\hat{\mu})\delta_{x-a\hat{\mu},y}}{2a} + m_f \delta_{x,y} \right) q^f(y)$$

Wilson term

This produces unphysical poles in the momentum-space propagator which need to be removed:

$$-\frac{1}{2a} \sum_{\mu=\pm1}^{\pm4} U_{\mu,ab}(x)\delta_{x+\hat{\mu},y} - 2\delta_{ab}\delta_{xy}$$

Improvement

- Discretisation of fermion and gluon action can be improved by adding higher-order terms in the expansion in a (the lattice spacing).
- These terms need to be renormalised (beyond the scope of this talk!)

Computing observables on the lattice

Observables defined through euclidean path integral:

$$\langle \mathcal{O} \rangle = \frac{1}{Z} \int \mathcal{D}[q,\bar{q}]\mathcal{D}[U] e^{-S_F[q,\bar{q},U]-S_G[U]} \mathcal{O}[q,\bar{q},U] \,.$$

Fermionic part: analytic solution by Grassmann integration

$$\langle \mathcal{O} \rangle = \frac{1}{Z} \int \mathcal{D}[U] e^{-S_G[U]} \det D[U] \underbrace{\mathcal{O}_F[U, G[U]]}_{\langle \mathcal{O} \rangle_F} \,.$$

Gluonic part: numerical solution by importance sampling of gauge configurations

$$\langle \mathcal{O} \rangle = \langle \langle \mathcal{O}_F \rangle \rangle_G = \lim_{N_{\text{cfgs}} \to \infty} \frac{1}{N_{\text{cfgs}}} \sum_{i=1}^{N_{\text{cfgs}}} \mathcal{O}_F[U_i, G[U_i]] \,.$$

Here we are interested in correlation functions of meson-interpolating operators:

$$\begin{aligned} C_{ij}(t) &\equiv \langle 0 | \mathcal{O}_i(t) \mathcal{O}_j^\dagger(0) | 0 \rangle \\ &= \sum_{n=1}^{\infty} \langle 0 | e^{Ht} \mathcal{O}_i(0) e^{-Ht} | n \rangle \langle n | \mathcal{O}_j^\dagger(0) | 0 \rangle \\ &= \sum_{n=1}^{\infty} e^{-E_n t} Z_i^n Z_j^{n*} \,, \end{aligned}$$

Spatial smearing: Distillation

- Jacobi smearing: $J(t;\sigma,n_\sigma) = \left(1+\frac{\sigma\nabla^2(t)}{n_\sigma}\right)^{n_\sigma}$
  Laplace operator: $\nabla^2_{xy}(t) = -6\delta_{xy} + \sum_{j=1}^{3}\left(U_j(x,t)\delta_{x+\hat{j},y} + U_j^\dagger(x-\hat{j},t)\delta_{x-\hat{j},y}\right)$

$$\lim_{n_\sigma\to\infty} J(t;\sigma,n_\sigma) = Q(t)\exp\left[\sigma\Lambda(t)\right]Q^\dagger(t)$$

- Distillation operator:

$$\left[\Box(t)\right]_{xy} = \left[V(t)V^\dagger(t)\right]_{xy} = \sum_{k=1}^{N} v_x^{(k)}(t)v_y^{(k)\dagger}(t)$$

  $V(t)$: first N column vectors of $Q(t)$; $\sigma = 0$

- Meson operator in distillation space:

$$C_M(t',t) = \langle \bar{q}'(t')\Box(t)\Gamma^B(t')\Box(t)q(t')\ \ \bar{q}(t)\Box(t)\Gamma^A(t)\Box(t)q'(t)\rangle$$
$$\to C_M^{\text{conn.}}(t',t) = \text{Tr}\left[\phi^B(t')\tau(t',t)\phi^A(t)\tau(t,t')\right].$$

- Distillation space objects:

$$\phi^X_{\alpha\beta}(t) = V^\dagger(t)\Gamma^X_{\alpha\beta}(t)V(t)$$
$$\tau_{\alpha\beta}(t',t) = V^\dagger(t')M^{-1}_{\alpha\beta}(t',t)V(t)$$

Ensembles

a_s	0.11 fm
a_t^{-1}	6.079 GeV
$(L/a_s)^3 \times (T/a_t)$	$32^3 \times 256$
m_π	239 MeV
N_f	$2+1$
N_{cfg}	484

a_s	0.12 fm
a_t^{-1}	5.667 GeV
$(L/a_s)^3 \times (T/a_t)$	$\{16^3, 20^3, 24^3\} \times 256$
m_π	391 MeV
N_f	$2+1$
N_{cfg}	$\{479, 603, 552\}$

$D\pi$ 239 MeV Operator Table (S-wave)

$A_1^+[000]$	$A_1[100]$	$A_1[110]$	$A_1[111]$	$A_1[200]$
$D_{[000]}\ \pi_{[000]}$	$D_{[000]}\ \pi_{[100]}$	$D_{[000]}\ \pi_{[110]}$	$D_{[000]}\ \pi_{[111]}$	$D_{[100]}\ \pi_{[100]}$
$D_{[100]}\ \pi_{[100]}$	$D_{[100]}\ \pi_{[000]}$	$D_{[100]}\ \pi_{[100]}$	$D_{[100]}\ \pi_{[110]}$	$D_{[110]}\ \pi_{[110]}$
$D_{[110]}\ \pi_{[110]}$	$D_{[100]}\ \pi_{[110]}$	$D_{[110]}\ \pi_{[000]}$	$D_{[110]}\ \pi_{[100]}$	$D_{[200]}\ \pi_{[000]}$
$D_{[111]}\ \pi_{[111]}$	$D_{[100]}\ \pi_{[200]}$	$D_{[110]}\ \pi_{[110]}$	$D_{[111]}\ \pi_{[000]}$	$D_{[210]}\ \pi_{[100]}$
$D_{[000]}\ \eta_{[000]}$	$D_{[110]}\ \pi_{[100]}$	$D_{[111]}\ \pi_{[100]}$	$D_{[211]}\ \pi_{[100]}$	$D_{[200]}\ \eta_{[000]}$
$D_{[100]}\ \eta_{[100]}$	$D_{[110]}\ \pi_{[111]}$	$D_{[210]}\ \pi_{[100]}$	$D^*_{[110]}\ \pi_{[100]}$	
$D_{s\,[000]}\ \bar{K}_{[000]}$	$D_{[111]}\ \pi_{[110]}$	$D^*_{[100]}\ \pi_{[100]}$	$D_{[111]}\ \eta_{[000]}$	
	$D_{[200]}\ \pi_{[100]}$	$D^*_{[111]}\ \pi_{[100]}$	$D_{s\,[111]}\ \bar{K}_{[000]}$	
	$D_{[210]}\ \pi_{[110]}$	$D_{[110]}\ \eta_{[000]}$		
	$D_{[000]}\ \eta_{[100]}$	$D_{s\,[110]}\ \bar{K}_{[000]}$		
	$D_{[100]}\ \eta_{[000]}$			
	$D_{s\,[000]}\ \bar{K}_{[100]}$			
	$D_{s\,[100]}\ \bar{K}_{[000]}$			
$8 \times \bar{\psi}\mathbf{\Gamma}\psi$	$18 \times \bar{\psi}\mathbf{\Gamma}\psi$	$18 \times \bar{\psi}\mathbf{\Gamma}\psi$	$9 \times \bar{\psi}\mathbf{\Gamma}\psi$	$16 \times \bar{\psi}\mathbf{\Gamma}\psi$

Operators used in the S-wave fits. Subscripts indicate momentum types. $\mathbf{\Gamma}$ represents some monomial of γ matrices and derivatives.

$D\pi$ 239 MeV Operator Table (P-wave)

T_1^- [000]	E_2 [100]	B_1 [110]	B_2 [110]
$D_{[100]}\ \pi_{[100]}$	$D_{[100]}\ \pi_{[110]}$	$D_{[100]}\ \pi_{[100]}$	$D_{[100]}\ \pi_{[111]}$
$D_{[110]}\ \pi_{[110]}$	$D_{[110]}\ \pi_{[100]}$	$D_{[110]}\ \pi_{[110]}$	$D_{[110]}\ \pi_{[110]}$
$D^*_{[100]}\ \pi_{[100]}$	$D^*_{[000]}\ \pi_{[100]}$	$D_{[210]}\ \pi_{[100]}$	$D_{[111]}\ \pi_{[100]}$
	$D^*_{[100]}\ \pi_{[000]}$	$D^*_{[100]}\ \pi_{[100]}$	$D^*_{[000]}\ \pi_{[110]}$
		$D^*_{[110]}\ \pi_{[000]}$	$D^*_{[100]}\ \pi_{[100]}\ \{2\}$
			$D^*_{[110]}\ \pi_{[000]}$
			$D^*_{[111]}\ \pi_{[100]}$
$6 \times \bar{\psi}\mathbf{\Gamma}\psi$	$18 \times \bar{\psi}\mathbf{\Gamma}\psi$	$18 \times \bar{\psi}\mathbf{\Gamma}\psi$	$20 \times \bar{\psi}\mathbf{\Gamma}\psi$

Operators used in the P-wave fits. Subscripts indicate momentum types. $\mathbf{\Gamma}$ represents some monomial of γ matrices and derivatives. The number in curly parentheses indicates the number of operators of this momentum combination.

$D^*\pi$ 391 MeV Operator Table (part 1)

$[000]\,T_1^+$	$[000]\,E^+$	$[000]\,T_2^+$	$[001]\,A_2$	$[001]\,E_2$	$[001]\,B_1$	$[001]\,B_2$
$D_{[000]}\rho_{[000]}$ (1)	$D_{[100]}\pi_{[100]}$ (1)	$D_{[110]}\pi_{[110]}$ (1)	$D_{[100]}\rho_{[000]}$ (1)	$D_{[100]}\pi_{[110]}$ (1)	$D_{[100]}\pi_{[110]}$ (1)	$D_{[111]}\pi_{[110]}$ (1)
$D_{[100]}\rho_{[100]}$ (2)	$D_{[110]}\pi_{[110]}$ (1)	$D^*{}_{[100]}\pi_{[100]}$ (1)	$D_{[000]}f_{0\,[100]}$ (1)	$D_{[110]}\pi_{[100]}$ (1)	$D_{[110]}\pi_{[100]}$ (1)	$D_{[110]}f_{0\,[100]}$ (1)
$D_{[100]}f_{0\,[100]}$ (1)	$D_{[200]}\pi_{[200]}$ (1)	$D^*{}_{[000]}\rho_{[000]}$ (1)	$D_{[100]}f_{0\,[000]}$ (1)	$D_{[111]}\pi_{[110]}$ (1)	$D_{[100]}\eta_{[110]}$ (1)	$D^*{}_{[100]}\pi_{[110]}$ (2)
$D^*{}_{[000]}\pi_{[000]}$ (1)	$D_{[100]}\eta_{[100]}$ (1)	$\bar{q}\mathbf{\Gamma}q$ (29)	$D^*{}_{[000]}\pi_{[100]}$ (1)	$D_{[110]}\eta_{[100]}$ (1)	$D_{[110]}\eta_{[100]}$ (1)	$D^*{}_{[110]}\pi_{[100]}$ (2)
$D^*{}_{[100]}\pi_{[100]}$ (2)	$D_{[110]}\eta_{[110]}$ (1)		$D^*{}_{[100]}\pi_{[000]}$ (1)	$D_{[000]}\rho_{[100]}$ (1)	$D_{s\,[100]}\bar{K}_{[110]}$ (1)	$\bar{q}\mathbf{\Gamma}q$ (20)
$D^*{}_{[110]}\pi_{[110]}$ (3)	$D_{s\,[100]}\bar{K}_{[100]}$ (1)		$D^*{}_{[110]}\pi_{[100]}$ (2)	$D_{[100]}\rho_{[000]}$ (1)	$D_{s\,[110]}\bar{K}_{[100]}$ (1)	
$D^*{}_{[000]}\eta_{[000]}$ (1)	$D_{s\,[110]}\bar{K}_{[110]}$ (1)		$D^*{}_{[100]}\eta_{[000]}$ (1)	$D_{s\,[110]}\bar{K}_{[100]}$ (1)	$\bar{q}\mathbf{\Gamma}q$ (12)	
$D^*{}_{[100]}\eta_{[100]}$ (2)	$\bar{q}\mathbf{\Gamma}q$ (4)		$D^*_{s\,[100]}\bar{K}_{[000]}$ (1)	$D^*{}_{[000]}\pi_{[100]}$ (1)		
$D^*{}_{[000]}\rho_{[000]}$ (1)			$D_{0\,[100]}\pi_{[000]}$ (1)	$D^*{}_{[100]}\pi_{[000]}$ (1)		
$D^*_{s\,[000]}\bar{K}_{[000]}$ (1)			$\bar{q}\mathbf{\Gamma}q$ (32)	$D^*{}_{[110]}\pi_{[100]}$ (3)		
$D^*_{s\,[100]}\bar{K}_{[100]}$ (2)				$D^*{}_{[000]}\eta_{[100]}$ (1)		
$D_{0\,[100]}\pi_{[100]}$ (1)				$D^*{}_{[100]}\eta_{[000]}$ (1)		
$\bar{q}\mathbf{\Gamma}q$ (44)				$D^*{}_{[100]}f_{0\,[000]}$ (1)		
				$D^*_{s\,[100]}\bar{K}_{[000]}$ (1)		
				$\bar{q}\mathbf{\Gamma}q$ (44)		

$I = 1/2$ $D^*\pi$-, $D^*\eta$- and $D^*_s\bar{K}$-like operators

$D^*\pi$ 391 MeV Operator Table (part 2)

$[000]\,T_1^-$	$[011]A_2$	$[011]B_1$	$[011]B_2$	$[111]A_2$	$[111]E_2$	$[002]A_2$
$D_{[100]}\pi_{[100]}$ (1)	$D_{[110]}\pi_{[110]}$ (1)	$D_{[100]}\pi_{[100]}$ (1)	$D_{[110]}\pi_{[110]}$ (1)	$D_{[111]}\rho_{[000]}$ (1)	$D_{[100]}\pi_{[110]}$ (1)	$D_{[100]}\rho_{[100]}$ (1)
$D_{[100]}\eta_{[100]}$ (1)	$D_{[110]}\rho_{[000]}$ (1)	$D_{[110]}\pi_{[110]}$ (1)	$D_{[111]}\pi_{[100]}$ (1)	$D_{[111]}f_{0\,[000]}$ (1)	$D_{[110]}\pi_{[100]}$ (1)	$D_{[100]}f_{0\,[100]}$ (1)
${D^*}_{[100]}\pi_{[100]}$ (1)	$D_{[110]}f_{0\,[000]}$ (1)	$D_{[210]}\pi_{[100]}$ (1)	$D_{[110]}\rho_{[000]}$ (1)	${D^*}_{[110]}\pi_{[100]}$ (2)	$D_{[211]}\pi_{[100]}$ (1)	$D_{[200]}f_{0\,[000]}$ (1)
$\bar{q}\mathbf{\Gamma}q$ (20)	${D^*}_{[100]}\pi_{[100]}$ (2)	$D_{[100]}\eta_{[100]}$ (1)	$D_{[100]}f_{0\,[100]}$ (1)	${D^*}_{[111]}\pi_{[000]}$ (1)	$D_{[100]}\eta_{[110]}$ (1)	${D^*}_{[100]}\pi_{[100]}$ (1)
	${D^*}_{[110]}\pi_{[000]}$ (1)	$D_{[110]}\rho_{[000]}$ (1)	${D^*}_{[000]}\pi_{[110]}$ (1)	${D^*}_{[111]}\eta_{[000]}$ (1)	$D_{[110]}\eta_{[100]}$ (1)	${D^*}_{[200]}\pi_{[000]}$ (1)
	${D^*}_{[111]}\pi_{[100]}$ (2)	$D_{s\,[100]}\bar{K}_{[100]}$ (1)	${D^*}_{[100]}\pi_{[100]}$ (2)	${D_s^*}_{[111]}\bar{K}_{[000]}$ (1)	$D_{[111]}\rho_{[000]}$ (1)	${D^*}_{[210]}\pi_{[100]}$ (2)
	${D^*}_{[110]}\eta_{[000]}$ (1)	${D^*}_{[000]}\pi_{[110]}$ (1)	${D^*}_{[110]}\pi_{[000]}$ (1)	$D_{0\,[111]}\pi_{[000]}$ (1)	$D_{[110]}f_{0\,[100]}$ (1)	${D^*}_{[100]}\eta_{[100]}$ (1)
	${D_s^*}_{[110]}\bar{K}_{[000]}$ (1)	${D^*}_{[100]}\pi_{[100]}$ (1)	${D^*}_{[111]}\pi_{[100]}$ (1)	$\bar{q}\mathbf{\Gamma}q$ (36)	$D_{s\,[100]}\bar{K}_{[110]}$ (1)	${D^*}_{[200]}\eta_{[000]}$ (1)
	$D_{0\,[110]}\pi_{[000]}$ (1)	${D^*}_{[110]}\pi_{[000]}$ (1)	${D^*}_{[110]}\eta_{[000]}$ (1)		$D_{s\,[110]}\bar{K}_{[100]}$ (1)	${D_s^*}_{[200]}\bar{K}_{[000]}$ (1)
	$\bar{q}\mathbf{\Gamma}q$ (52)	${D^*}_{[111]}\pi_{[100]}$ (2)	${D_s^*}_{[110]}\bar{K}_{[000]}$ (1)		${D^*}_{[100]}\pi_{[110]}$ (3)	$\bar{q}\mathbf{\Gamma}q$ (32)
		${D^*}_{[100]}\eta_{[100]}$ (1)	$\bar{q}\mathbf{\Gamma}q$ (52)		${D^*}_{[110]}\pi_{[100]}$ (3)	
		${D^*}_{[110]}\eta_{[000]}$ (1)			${D^*}_{[111]}\pi_{[000]}$ (1)	
		${D^*}_{[110]}f_{0\,[000]}$ (1)			${D^*}_{[111]}\eta_{[000]}$ (1)	
		${D_s^*}_{[110]}\bar{K}_{[000]}$ (1)			${D_s^*}_{[111]}\bar{K}_{[000]}$ (1)	
		$\bar{q}\mathbf{\Gamma}q$ (44)			$\bar{q}\mathbf{\Gamma}q$ (60)	

$I = 1/2$ $D^*\pi$-, $D^*\eta$- and $D_s^*\bar{K}$-like operators

Subduction Table (1)

$\vec{P}$	Irrep Λ	J^P ($\vec{P}=\vec{0}$) $\lvert\lambda\rvert^{(\tilde{\eta})}$ ($\vec{P}\neq\vec{0}$)	$D\pi$ $J^P_{[N]}$	$D^*\pi$ $J^P_{[N]}$
[000]	A_1^+	0^+, 4^+	0^+, ...	...
	T_1^-	1^-, 3^-	1^-, ...	...
	E^+	2^+, 4^+	2^+, ...	...
[n00]	A_1	$0^{(+)}$, 4	0^+, 1^-, 2^+, ...	...
	E_2	1, 3	1^-, 2^+, ...	1^+, ...
[nn0]	A_1	$0^{(+)}$, 2, 4	0^+, 1^-, $2^+_{[2]}$, ...	...
	B_2, B_2	1, 3	1^-, 2^+, ...	1^+, ...
[nnn]	A_1	$0^{(+)}$, 3	0^+, 1^-, 2^+, ...	...

Lowest $D\pi$ and $D^*\pi$ continuum J^P and helicity λ subductions by irrep

Subduction Table (2)

$\vec{d}$	G	Λ	J^P $(\vec{P}=\vec{0})$ $\lvert\lambda\rvert^{(\tilde{\eta})}$ $(\vec{P}\neq\vec{0})$	${}^1\ell_J$	${}^3\ell_J$
[000]	O_h	A_1^+	0^+, ...	${}^1S_0$	
		A_2^+	3^+, ...		${}^3D_3$
		E^+	2^+, ...	${}^1D_2$	${}^3D_2$
		T_1^+	1^+, 3^+, ...		$({}^3S_1, {}^3D_1)$, ${}^3D_3$
		T_2^+	2^+, ...	${}^1D_2$	${}^3D_2$, ${}^3D_3$
		A_1^-	0^-, ...		${}^3P_0$
		A_2^-	3^-, ...	...	...
		E^-	2^-, ...		${}^3P_2$
		T_1^-	1^-, 3^-, ...	${}^1P_1$	${}^3P_1$
		T_2^-	2^-, ...		${}^3P_2$
$[n00]$	C_{4v}	A_2	$0^{(-)}$, $1^{(+)}$, $2^{(-)}$, $3^{(+)}$		${}^3P_0$, $({}^3S_1, {}^3D_1)$, ${}^3P_2$, ${}^3D_3$
		B_1, B_2	2, 3	${}^1D_2$	${}^3D_2$, ${}^3P_2$, ${}^3D_2$
		E_2	1, 2, 3	${}^1P_1$, ${}^1D_2$	$({}^3S_1, {}^3D_1)$, ${}^3P_1$, ${}^3D_2$, ${}^3P_2$, ${}^3D_3$
$[nn0]$	C_{2v}	A_2	$0^{(-)}$, $1^{(+)}$, 2, 3	${}^1D_2$	${}^3P_0$, $({}^3S_1, {}^3D_1)$, ${}^3D_2$, ${}^3P_2$, ${}^3D_3$
		B_1, B_2	1, 2, 3	${}^1P_1$, ${}^1D_2$	$({}^3S_1, {}^3D_1)$, ${}^3P_1$, ${}^3D_2$, ${}^3P_2$, ${}^3D_3$
$[nnn]$	C_{3v}	A_2	$0^{(-)}$, $1^{(+)}$, 2^-, 3		${}^3P_0$, $({}^3S_1, {}^3D_1)$, ${}^3P_2$, ${}^3D_3$
		E_2	1, 2, 3	${}^1P_1$, ${}^1D_2$	$({}^3S_1, {}^3D_1)$, ${}^3D_2$, ${}^3P_2$, ${}^3D_3$

Lattice symmetry groups and partial-wave subductions for vector-pseudoscalar scattering

Masses and thresholds ($m_\pi = 239$ MeV)

	$a_t m$
π	0.03928(18)
K	0.08344(7)
η	0.09299(56)
D	0.30923(11)
D_s	0.32356(12)
D^*	0.33058(24)

	$a_t E_{\mathrm{threshold}}$
$D\pi$	0.34851(21)
$D\pi\pi$	0.38779(27)
$D\eta$	0.40222(57)
$D_s\bar{K}$	0.40700(14)
$D^*\pi\pi$	0.40914(35)

Left: Stable hadron masses. Right: kinematic thresholds.

Masses and thresholds ($m_\pi = 391$ MeV)

	$a_t m$
π	0.06906(13)
K	0.09698(9)
η	0.10364(19)
D	0.33303(31)
D_s	0.34441(29)
D^*	0.35494(46)
D_s^*	0.36587(35)

	$a_t E_{\text{threshold}}$	$E_{\text{threshold}}$/MeV
$D\pi$	0.40209(34)	2278.6 ± 1.9
$D^*\pi$	0.4240(5)	2402.8 ± 2.7
$D^*\eta$	0.4586(5)	2598.8 ± 2.8
$D_s^*\bar{K}$	0.4629(4)	2623.0 ± 2.0
$D\pi\pi$	0.4711(4)	2670.0 ± 2.3
$D^*\pi\pi$	0.4931(5)	2794.2 ± 3.0

Left: Stable hadron masses. Right: kinematic thresholds.

Operator basis variations

- Varying the basis affects the spectrum
- $I = 1/2$ allows both meson-meson and $q\bar{q}$-like operator constructions
- Interpolating the complete spectrum requires both types of operator
- Other meson-meson operators do not play a significant role below coupled-channel threshold

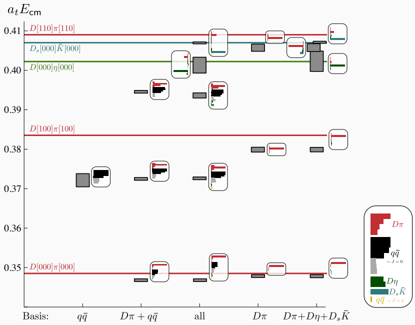

Spectrum in A_1^+

1D QM: 1 boson

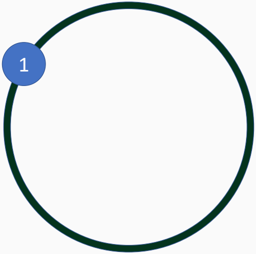

Picture 1 boson in a periodic one-dimensional volume:

- Periodic boundary conditions: $\psi(0) = \psi(L)$ and $\psi'(0) = \psi'(L)$
- $\psi(x) \sim e^{ipx}$
- Momentum quantised: $p_n = \frac{2\pi n}{L}$
- Discrete energy spectrum: $E_n = \sqrt{m^2 + p_n^2}$
  $\rightarrow$ depends on size of box

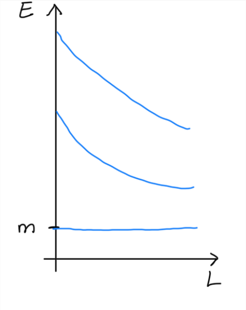

1D QM: 2 bosons, no interaction

Now picture 2 (non-interacting) bosons in the same volume:

- Periodic boundary conditions: $\psi(0) = \psi(L)$ and $\psi'(0) = \psi'(L)$
- $\psi(x) \sim e^{ipx}$ $(x = x_1 - x_2)$
- COM momentum quantised: $p_n = \frac{2\pi n}{L}$
- Discrete energy spectrum: $E_{n,m} = \sqrt{m_1^2 + p_n^2} + \sqrt{m_2^2 + p_n^2}$ $\rightarrow$ depends on size of box

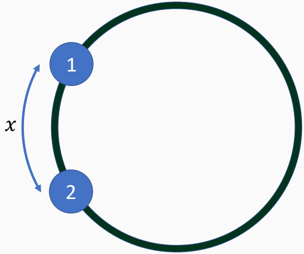

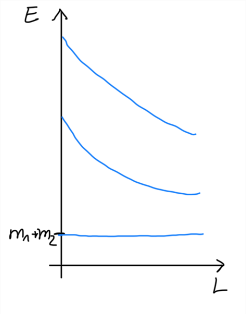

1D QM: 2 bosons, finite-range potential

Now turn on interactions:

- Periodic boundary conditions: $\psi(0) = \psi(L)$ and $\psi'(0) = \psi'(L)$
- $\psi_{\text{out}}(x) \sim e^{ipx+\delta(p)}$ (far from interaction, $x = x_1 - x_2$)
- Momentum quantised and shifted: $p_n = \frac{2\pi n}{L} - \frac{2}{L}\delta(P)$
- Discrete energy spectrum depends on volume and interaction: $E_n = E_n(\delta, L)$
- The energies are shifted w.r.t. the non-interacting case

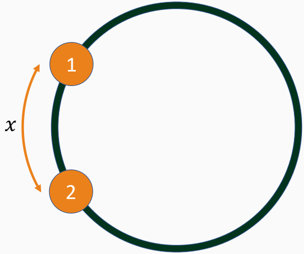

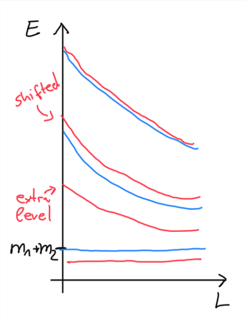

$D\pi$ at $m_\pi = 239$ MeV: Spectra

Lattice study of $D\pi \to D\pi$ scattering with $m_\pi = 239$ MeV:

- Energies extracted from fit of sum of exponentials to principal correlators
- Irreps labelled $[\vec{d}]\Lambda^{(P)}$ (overall momentum $\vec{P} = 2\pi\vec{d}/L$)
- At $\vec{P} = \vec{0}$:
  - $A_1^+ \leftrightarrow S$-wave
  - $T_1^- \leftrightarrow P$-wave
- Threshold suppression $\propto k^{2l}$: higher partial waves may be neglected
- Non-zero momentum $\to$ more mixing of partial waves

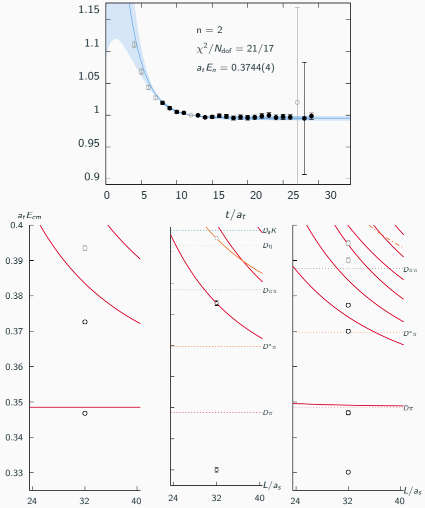

$[000]A_1^+$ $[000]T_1^-$ $[100]A_1$

$D\pi$ at $m_\pi = 239$ MeV: Operator basis variations

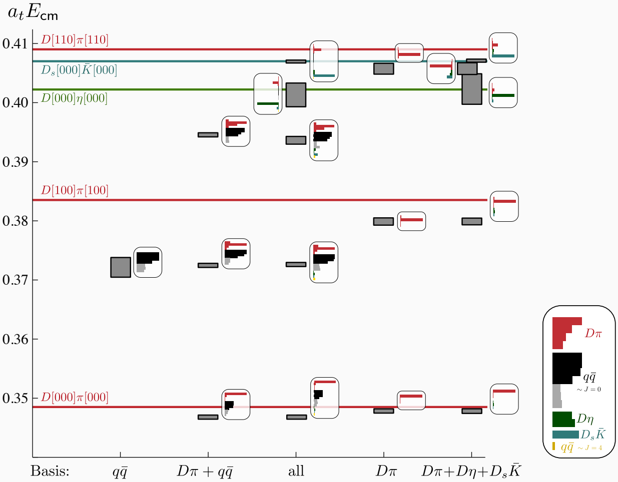

Spectrum in A_1^+

→ A stable spectrum requires both $q\bar{q}$- and meson-meson-like operators!

$D\pi$ at $m_\pi = 239$ MeV: Parametrisations and poles

$\ell=0$ parameterisation	$\ell=1$ parameterisation	N_{pars}	χ^2/N_{dof}
K-matrix with Chew-Mandelstam $I(s)$ in both partial waves			
ref. $K = \frac{g^2}{m^2-s} + \gamma^{(0)}$	$K = \frac{g_1^2}{m_1^2-s}$	5	0.90
(a) $K = \frac{g^2}{m^2-s}$	$K = \frac{g_1^2}{m_1^2-s}$	4	0.90
(b) $K = \frac{g^2}{m^2-s} + \gamma^{(1)}\hat{s}$	$K = \frac{g_1^2}{m_1^2-s}$	5	0.90
(c) $K = \frac{(g+g^{(1)}s)^2}{m^2-s}$	$K = \frac{g_1^2}{m_1^2-s}$	5	0.90
(d) $K^{-1} = c^{(0)} + c^{(1)}\hat{s}$	$K = \frac{g_1^2}{m_1^2-s}$	4	0.90
(e) $K^{-1} = \frac{c^{(0)}+c^{(1)}\hat{s}}{c^{(2)}\hat{s}}$	$K = \frac{g_1^2}{m_1^2-s}$	5	0.90
(f) $K = \frac{g^2}{m^2-s} + \gamma^{(0)} + \gamma^{(1)}\hat{s}$	$K = \frac{g_1^2}{m_1^2-s}$	6	*0.94**
K-matrix with $I(s) = -i\rho(s)$ in both partial waves			
(g) $K = \frac{g^2}{m^2-s} + \gamma^{(0)}$	$K = \frac{g_1^2}{m_1^2-s}$	5	0.90
(h) $K = \frac{g^2}{m^2-s}$	$K = \frac{g_1^2}{m_1^2-s}$	4	0.91
(i) $K = \frac{(g+g^{(1)}s)^2}{m^2-s}$	$K = \frac{g_1^2}{m_1^2-s}$	5	0.90
(j) $K^{-1} = c^{(0)} + c^{(1)}\hat{s}$	$K = \frac{g_1^2}{m_1^2-s}$	4	0.91
(k) $K^{-1} = \frac{c^{(0)}+c^{(1)}\hat{s}}{c^{(2)}\hat{s}}$	$K = \frac{g_1^2}{m_1^2-s}$	5	0.90
K-matrix with Chew-Mandelstam $I(s)$ in S-wave, Effective range in P-wave			
(l) $K = \frac{g^2}{m^2-s} + \gamma^{(0)}$	$k\cot\delta_1 = 1/a_1 + \frac{1}{2}r_1^2k^2$	5	0.93
Effective range in S wave, K-matrix with Chew-Mandelstam $I(s)$ in P-wave			
(m) $k\cot\delta_0 = 1/a_0 + \frac{1}{2}r_0^2k^2$	$K = \frac{g_1^2}{m_1^2-s}$	4	0.93
(n) $k\cot\delta_0 = 1/a_0 + \frac{1}{2}r_0^2k^2 + P_{2,0}k^4$	$K = \frac{g_1^2}{m_1^2-s}$	5	*0.88†*
Effective range in both partial waves			
(o) $k\cot\delta_0 = 1/a_0 + \frac{1}{2}r_0^2k^2$	$k\cot\delta_1 = 1/a_1 + \frac{1}{2}r_1^2k^2$	4	0.93
(p) $k\cot\delta_0 = 1/a_0 + \frac{1}{2}r_0^2k^2 + P_{2,0}k^4$	$k\cot\delta_1 = 1/a_1 + \frac{1}{2}r_1^2k^2$	5	*0.91†*
Breit-Wigner in S-wave, K-matrix with Chew-Mandelstam $I(s)$ in P-wave			
(q) $t = \frac{1}{\rho}\frac{m_R\Gamma_0}{m_R^2-s-im_R\Gamma_0}$	$K = \frac{g_1^2}{m_1^2-s}$	4	0.91
First-order unitarised χ_{PT}			
(s) $t^{-1} = \left(-\frac{1}{16\pi}\mathcal{V}_{J=0}\right)^{-1} + 16\pi G_{\text{DR}}$	$K = \frac{g_1^2}{m_1^2-s}$	4	0.86

[L. Gayer, N. Lang et al (HadSpec), arXiv:2102.04973]

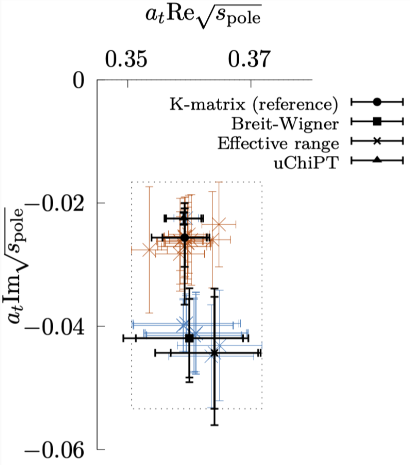

$I = 0$ DK at $m_\pi = 239$ MeV and $m_\pi = 391$ MeV

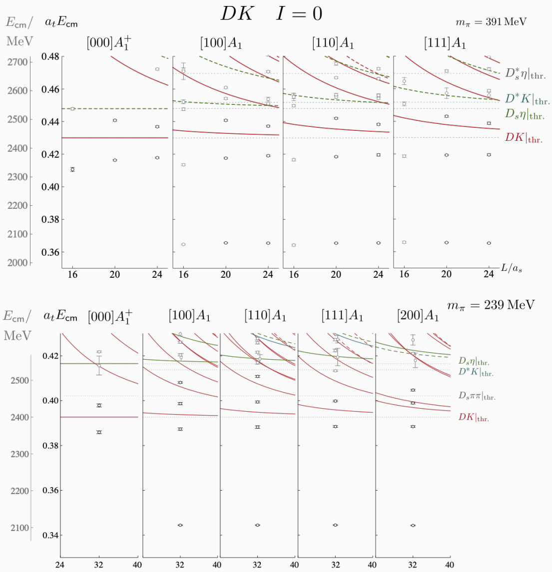

[G. Cheung et al (HadSpec), JHEP 02 (2021) 100 arXiv: 2008.06432]

SU(3) point

Consider $SU(3)_F$ symmetric theory $(m_u = m_d = m_s)$:

- meson-meson system transforms like $\bar{\mathbf{3}} \otimes \mathbf{8} = \bar{\mathbf{3}} \oplus \mathbf{6} \oplus \overline{\mathbf{15}}$ under flavour rotations
- For broken flavour symmetry these representations mix: $D^{(*)}\pi$ / $D^{(*)}\eta$ / $D_s^{(*)}\bar{K}$ receive contributions from all three

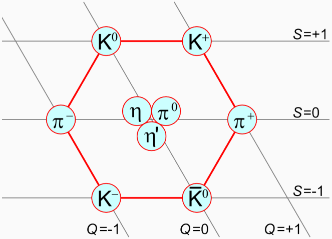

https://en.wikipedia.org/wiki/Quark_model - Public Domain